Oxygen Redox Reaction in Lithium-based Electrolytes: from Salt-in-Solvent to Solvent-in-Salt

Oxygen Redox Reaction in Lithium-based Electrolytes: from Salt-in-Solvent to Solvent-in-Salt

Francesca Messaggi[a], Irene Ruggeri[a,1], Damiano Genovese[a], Nelsi Zaccheroni[a], Catia Arbizzani[a,1], Francesca Soavi[a,1,*]

[a]Department of Chemistry, Alma Mater Studiorum-Bologna University, Via F. Selmi 2, 40126, Bologna, Italy

[1] ISE members

*Francesca Soavi, Department of Chemistry "Giacomo Ciamician" Alma Mater Studiorum-Bologna University, Via F. Selmi 2, 40126, Bologna, Italy. Tel.: +39 0512099797; fax: +39 0512099365; e-mail: francesca.soavi@unibo.it

Abstract

Electrolytes are key components of Li/O_2 batteries. The ionic liquid-like structure and good electrochemical and thermal stability of solvent-in-salt electrolytes make them of great interest for lithium batteries. Solutions of lithium bis(trifluoromethanesulfonyl)imide in tetraethylene glycol dimethyl-ether with molar ratios ranging from 1:9 to 1:0.9 are here investigated. A voltammetric study of oxygen redox reaction in presence of different concentrations of salt, from salt-in-solvent to solvent-in-salt solutions, is reported here for the first time along with a novel luminescence method for the evaluation of O_2 solubility. The results indicate that superconcentrated solutions favor the solution formation mechanism of Li_2O_2 during discharge

which in turn is beneficial for battery cycling stability. Despite the higher viscosity of solvent-in-salt solutions than conventional electrolytes, O_2 solubility is improved at the highest salt concentrations. These findings contribute to understand electrochemical processes in solvent-in-salt solutions for Li/O_2 and next generation metal-based batteries.

Keywords: Cyclic voltammetry; oxygen redox reaction; solvent-in-salt solution; Li/O_2 battery; superconcentrated solution; oxygen solubility; luminescence quenching.

1. Introduction

In recent years, the very high theoretical specific energy of Li/O_2 batteries, comparable to gasoline value, has attracted the interest of researchers [1]. The oxygen redox reaction (ORR) in non-aqueous electrolytes involves the formation of lithium superoxide (LiO_2) that evolves to lithium peroxide (Li_2O_2) via chemical disproportion and electrochemical processes [2]. Discharge products and mainly superoxide are highly reactive species that cause electrolyte and carbon cathode degradation [3-5]. Insoluble Li_2O_2 clogs the cathode surface during battery discharge and brings about high recharge overpotentials. Battery cycling stability is, therefore, affected by electrolyte chemical and electrochemical stability and by the electrode passivation with solid Li_2O_2 [6, 7]. Electrolytes in Li/O_2 batteries have to be resistant towards the superoxide ($O_2^{\cdot-}$) and peroxide (O_2^{2-}) ions formed during discharge, should feature good oxidative resistance, high O_2 solubility and mass transport, and should be engineered in order to promote the Li_2O_2 solution formation mechanism vs. the surface growth [6, 8-11]. Indeed, the formation in solution of Li_2O_2 particles that, then, agglomerate on the electrode as large clusters keeps part of the

carbon surface free from passivation. This enables high discharge capacities. Instead, surface growth mechanism produces highly passivating thin film on electrode surface that accelerates cell death [3, 6, 12]. The two mechanisms are driven by the stability of the superoxide anion in solution, which in turn depends on solvent donor number (DN) and on electrolyte cation Lewis acidity [13,14]. High-DN solvents and soft Lewis acid cations promote the solution mechanism and stabilize the superoxide (soft Lewis base). Low-DN solvents and hard Lewis acid cations, like free Li^+ ions, facilitate the surface mechanism and superoxide disproportionation to peroxide (hard Lewis base) [6, 12, 15, 16]. Solution of lithium bis(trifluoromethanesulfonyl)imide (LiTFSI) in tetraethylene glycol dimethyl-ether (TEGDME) and 1-butyl-1-methylpyrrolidinium bis(trifluoromethanesulfonyl)imide ($PYR_{14}TFSI$) ionic liquid (IL) are known for their wide electrochemical stability window, high chemical oxidation stability, high compatibility with Li metal, high Li^+ ion transport rate and good oxygen transport properties, which are key features for a Li/O_2 battery [17,18]. TEGDME is of particular interest for its low dielectric constant that favors oxygen solubility [19]. Table 1S compares dielectric constant, viscosity, O_2 solubility and DN of solvents commonly used in lithium battery electrolyte formulations. Recently, "solvent-in-salt" (SIS) solutions, featuring salt-to-solvent ratio in weight or volume greater than 1, have been proposed as key electrolytes for lithium batteries, including Li/S and Li/O_2 batteries [20-24]. Mandai et al. proposed SIS electrolytes based on LiTFSI in TEGDME and demonstrated that when the salt-to-solvent molar ratio approaches 1:1 the solutions have an IL-like structure with independent $[Li(glyme)_1]^+$ cation complexes and $TFSI^-$ anions, as shown in the right side of Figure 1 [25].

<Figure 1 >

Li et al. explored solutions with different LiTFSI-to-TEGDME molar ratios in the range 1:7 to 1:1 in Li/O_2 cells [22]. The best capacity retention and discharge voltage stability was achieved at the 1:5 ratio, out of the SIS range. This ratio was considered the best compromise to alleviate the reactivity of $O_2^{\cdot-}$ with both the free glyme (at lower molar ratios) and the glyme of the $[Li^+(glyme)_1\cdots O_2^{\cdot-}]$ complex (at higher molar ratios). The study mainly relied on galvanostatic charge/discharge performance of 2-electrode Li/O_2 cells, where both cathode and anode processes play a role. Lithium is expected to affect cell performance, too, and solid electrolyte interface (SEI) stability at the lithium metal anode has been demonstrated to improve by the use of SISs [23,24]. However, the work by Li et al. did not include a specific electrochemical study of cathode ORR reactions [22].

There is no general acceptance on the mechanism of ORR in a wide range of salt concentrations in aprotic solvents. This work addresses this issue by a voltammetric study in LiTFSI-TEGDME solutions in both the salt-in-solvent and SIS regions. The study is supported by a luminescence method for the evaluation of O_2 solubility.

2. Experimental

2.1 Materials and chemical-physical characterization of the solutions

Lithium bis(trifluoromethanesulfonyl)imide (LiTFSI, ≥99%, Aldrich) and tetraethylene glycol dimethyl ether (TEGDME, 99%, Aldrich, 20 ppm of H_2O) were both used as received. The LiTFSI-TEGDME solutions were prepared and stored in dry box (MBraun, O_2 and H_2O < 1 ppm). The physical chemical characterization comprises density and viscosity measurements, ionic conductivity tests and thermogravimetric analyses. The density was calculated after weighting three volumetric flasks with 5 mL of each solution (class A glassware, uncertainty ±

0.025 ml) at a temperature of 22°C ± 1°C and atmospheric pressure (0.1 ± 0.01 MPa). Viscosity was measured using a ViscoClock unit combined with a Micro-Ubbelohde viscometer (SI Analytics) at 22°C ± 1°C and atmospheric pressure (0.1 ± 0.01 MPa). A capillary with a diameter of 0.53 mm was used for solutions from 0 to 2 m, instead a larger capillary (Ø 0.96 mm) was used from 3 m to 5 m solutions. The accuracy on the flow time is 0.01% with 95% confidence level. Ionic conductivity was investigated in the range -20°C/80°C. It was measured by CDM 210 Conductivity Meter (MeterLab) with an Amel standard cell (platinum electrodes). The temperature was controlled by a Haake DC50 K40 thermocryostat with an accuracy of 0.1°C. Samples were thermostated for 1h before every measurement. Thermal weight loss temperature was detected with a TA Instruments Q50 thermogravimetric apparatus. Every sample was heated from room temperature to 500°C at the scan rate of 10 °C/min under argon flow. The instrument sensitivity is of 0.1 μg.

2.2 Electrochemical study

ORR in different electrolytes was investigated by cyclic voltammetry at glassy carbon electrode (GCE, 3 mm diameter) in a 5 mL cell that was thermostated at 30 °C by a Huber CC304 thermostat. The GC was polished with alumina paste on a Selvyt cloth before each scan, except for the stability test when the experiments were run continuously. A Li counter electrode (separated from the solution by a porous frit) was used while the reference electrode was a silver wire in $6x10^{-2}$ M AgTFSI (97%, Aldrich)-$PYR_{14}TFSI$; the reference electrode potential was checked vs. lithium and the working potentials are reported vs. the Li^+/Li couple. Oxygen (>99.999%, SIAD) was bubbled through the cell for at least 30 min before starting the analyses and was continuously flowed during the experiment. The electrochemical tests were performed

with a PerkinElmer VSP multichannel potentiostat/galvanostat. The voltammetric scans were corrected for the uncompensated resistance which was evaluated by electrochemical impedance spectroscopy at 10 kHz.

Galvanostatic measurements were performed with carbon paper (CP, Spectracarb 2050, Spectracorp, 0.5 cm^2) working electrodes dried under vacuum at 120°C overnight before use. During the measurement, the electrolyte was stirred and continuously fed with O_2.

2.3 Oxygen solubility by luminescence lifetime analysis

Oxygen solubility in LiTFSI-TEGDME electrolytes was evaluated by exploiting tris(2,2′-bipyridyl)dichlororuthenium(II) hexahydrate ($Ru(bpy)_3Cl_2$, 99.95%, Aldrich) as a probe [26, 27]. This very well-known metal complex presents a luminescence centred ad 610 nm (in water), with a metal to ligand charge transfer (MLCT) and triplet character. The luminescence intensity and lifetime are largely affected by the presence of molecular oxygen in solution that acts as a quencher [28, 29]. If luminescence quenching is purely diffusional, the luminescence lifetime (and intensity) is determined by the quencher concentration following a relation quantitatively expressed by the Stern-Volmer equation (Eq. 1) [30]:

$$\frac{\tau}{\tau_0} = 1 + k_q \tau_0 [O_2] \quad (1)$$

where τ and τ_0 are the lifetime of the luminophore in presence and absence of the quencher, respectively, and k_q is the quenching constant. Quenching is strongly influenced by diffusion of the quencher (O_2) and luminophore, in turn related to the viscosity of the sample by the Stokes-Einstein equation. The quenching constant corrected for the diffusional terms is described by Eq. (2).

$$k_q = \gamma \left[N_A \frac{2}{3} k_B (R_f + R_q) \left(\frac{1}{R_f} + \frac{1}{R_q} \right) \right] \frac{T}{\eta} \quad (2)$$

where γ is the quantic efficiency, close to 1 for a quencher like O_2, N_A is the Avogadro number, k_B the Boltzmann constant, R_f and R_q the radii of the metal complex ($Ru(bpy)_3^{2+}$, $6.5 \cdot 10^{-10}$ m) and the quencher (O_2, $1.21 \cdot 10^{-10}$ m), T the absolute temperature, and η the viscosity. The Stokes-Einstein equation holds only for viscosities lower than 125 cP, therefore equation (2) was not used for the 5m solution case [30-32].

The optical measurements were made in solutions of 10^{-5} M $Ru(bpy)_3Cl_2$ in 0, 0.5, 1, 2, 3 and 5 molal LiTFSI-TEGDME electrolytes. The quenching experiments were carried out after bubbling O_2 for 30 minutes into the cuvette containing Ru complex. Luminescence decay was found not to show further changes upon longer O_2 exposure time. UV-vis absorption spectra were recorded at 25 °C by means of Perkin-Elmer Lambda 45 spectrophotometer. Quartz cuvettes with optical path length of 1 cm were used. The fluorescence spectra were recorded with an Edinburgh FLS920 equipped with a photomultiplier Hamamatsu R928P. The same instrument connected to a PCS900 PC card was used for the TCSPC experiments to record the time-resolve emission decay [33].

3. Results and Discussion

Table 1 reports the salt concentrations and salt-to-solvent molar ratios of the investigated solutions, i.e. 0.5, 2.0, 4 and 5 mol/kg corresponding to 1:9, 1:2.3, 1:1.1 and 1:0.9 molar ratios, along with the corresponding density, viscosity, and conductivity values at room temperature and thermal weight loss temperature. The LiTFSI:TEGDME molar ratio of the 4m solution is 1:1.1, therefore a 10% excess of glyme vs. Li^+ is present. The molar ratio of the 5m solution is 1:0.9 which means there is a 10% excess of LiTFSI vs. solvent. These differences in the molar ratios

dramatically affected viscosity while keeping ionic conductivity at good values. Indeed, the conductivity at room temperature changes from 1.4 mS/cm for the 4m solution to 0.7 mS/cm for the 5m electrolyte, with a change of viscosity from 90 cP to 550 cP, respectively. Noticeably, the ion conductivity of the 5m solution, despite its high viscosity, is of the same order of magnitude of that of the salt-in-solvent solutions presenting viscosities in the range 7-90 cP. This experimental evidence suggests that the peculiar IL-like structure of the SIS solutions may bring about different ion conduction mechanisms with respect to classical electrolytes [20, 21, 23].

<Table 1>

Cyclic voltammetry is a powerful tool to get insight into ORR process mechanisms. Cyclic voltammetries were carried out with a glassy carbon electrode (GCE) in O_2 saturated solutions and the cyclic voltammograms (CVs) at 20 mV s^{-1} are reported in Figure 2; Table 2 reports key CV parameters and summarizes the reduction and oxidation potentials, currents and charge in 0.1, 0.5, 2, 4 and 5 molal LiTFSI-TEGDME.

<Figure 2>

<Table 2>

The CVs have almost the same shape and they reveal that ORR is electrochemically irreversible in all the investigated TEGDME-LiTFSI solutions. The reduction peak around 2 V vs Li^+/Li is

related to O_2 reduction to superoxide (eq. 3), which in turn gives Li_2O_2 by chemical dismutation (eq. 4) and/or electrochemical reduction (eq. 5):

$$O_2\ (sol) + e^- + Li^+\ (sol) \leftrightarrow LiO_2\ (sol) \quad (3)$$

$$2\ LiO_2\ (sol) \rightarrow Li_2O_2\ (s) + O_2\ (sol) \quad (4)$$

$$LiO_2\ (sol) + e^- + Li^+\ (sol) \rightarrow Li_2O_2\ (s) \quad (5)$$

The broad oxidation peak around 3.5 V vs Li^+/Li is attributed to Li_2O_2 reoxidation to O_2 (eq. 6)[34]:

$$Li_2O_2\ (s) \rightarrow O_2\ (sol) + 2\ Li^+\ (sol) + 2\ e^- \quad (6)$$

The presence of both electrochemical and chemical steps makes the study of ORR in the investigated electrolytes challenging. It requires an in depth analysis of the evolution of the processes moving from low to high concentrated solutions. Such analysis can be performed by studying the evolution of the CV peak potentials and currents.

The CVs reported in Figure 2a for 0.1, 0.5 and 2m LiTFSI-TEGDME show a shift of the reduction wave to more positive potentials and an increase of $I_{p,red}$. In oxidation, there is a small shift of the wave towards more negative values while $I_{p,ox}$ still increases. These trends, and specifically the E_{red} shift, are attributed to the increase of Li^+ concentration and explained referring to the Li^+ hard Lewis acidity. According to the Hard Soft Acid Base (HSAB) theory, soft Lewis acid cations stabilize the soft Lewis base superoxide anion while hard Lewis acid cations, like Li^+, have an higher affinity with hard Lewis bases like O_2^{-2} and promotes superoxide dismutation to peroxide (eq. 4). Therefore, ORR is a quasi-reversible monoelectronic

process involving the $O_2/O_2^{\cdot-}$ redox couple in Li^+ free electrolytes featuring soft Lewis base cations. This is the case of ORR in IL like $PYR_{14}TFSI$, where O_2 reduction takes place at 1.75 V vs Li^+/Li and reoxidation is at 1.9 V vs Li^+/Li (Figure 1S). Superoxide is unstable in presence of lithium salt and a chemical reaction, i.e. superoxide dismutation to peroxide, follows the first electrochemical reduction step (eq. 3) bringing about the formation of insulating Li_2O_2 on the electrode (eq. 4) [34-36]. The overall results are: i) ORR becomes electrochemically irreversible, ii) the main CV reduction peak potential E_{red} is shifted to more positive values (as expected for chemical reactions following the electrochemical step), iii) CV peak currents decrease, and iv) the superoxide oxidation peak disappears being replaced by the broader peroxide oxidation peak displaced towards more positive potentials [37]. This is clearly highlighted by the comparison of the CVs obtained in $PYR_{14}TFSI$ with and without LiTFSI that are reported in Figure 1S. Accordingly, it can be argued that the anticipation of the reduction wave moving from 0.1m to 0.5m LiTFSI in TEGDME (Figure 2a) is due to the increase of Li^+ concentration that favors the chemical dismutation reaction (eq. 4) that follows the electrochemical step (eq.3) and that yields O_2 (sol) and Li_2O_2(s). This takes also to other two consequences: i) to a higher O_2 concentration at the electrode/electrolyte interface with respect to the bulk and, hence, to a higher $I_{p,red}$ (like in an irreversible catalytic reaction, following a reversible charge transfer) [38] and ii) to a higher amount of Li_2O_2 (s) that can be reoxidized during the following anodic scan. This also brings about ~~formed during O_2 reduction determining the enhancement of~~ higher $I_{p,ox}$ currents because Li_2O_2 is the oxidation reaction reactant (eq. 6).

It has to be highlighted, however, that the E_{red} and $I_{p,red}$ of the CVs in 2m LiTFSI do not differ from those in the 0.5m solution. Unexpected results are also obtained with more concentrated solutions. Figure 2b reports the CVs obtained in 2m, 4m and 5m electrolytes. At 4m and 5m

LiTFSI, the E_{red} shifts towards more negative values and $I_{p,red}$ decreases with respect to the 2m and 0.5m cases (cfr. Figure 2b and Figure 2a). This can be explained by taking into account that Li^+ ion complexation by glyme molecules starts to be effective. Even if more Li^+ cations are present with respect to the 0.5m, their Lewis acidity is softened by glyme coordination. The $[Li(glyme)_1]^+$ complex stabilizes superoxide and makes the chemical dismutation less pronounced. Consequently, the amounts of O_2 and Li_2O_2 that are produced at the electrode interface by chemical disproportion (eq. 4) are lower. Given that in the 4m and 5m solutions the amount of the reduction reactant at the electrode surface, i.e. O_2, is lower, the values of the reduction currents $I_{p,red}$ are lower, too, as shown by the CVs in Figure 2b.

On the other hand, the oxidation currents $I_{p,ox}$ are related to the amount of the oxidation reactant, i.e. Li_2O_2 deposited/adsorbed at the electrode surface, which in turns relates to superoxide stability (eq 4) and to electrolyte viscosity. The notable increase of viscosity moving from 0.5m to 2m solutions (7 cP and 31 cP, respectively, see Table 1) causes the confinement of Li_2O_2 near the electrode surface and the increase of $I_{p,ox}$ (Figure 2a). At concentrations higher than 2m (Figure 2b), $I_{p,ox}$ does not change because the lower amount of Li_2O_2 at the electrode surface, formed by eq. 4, is balanced by the higher solution viscosity which impedes diffusion of Li_2O_2 from the electrode to the electrolyte bulk.

The higher stability of superoxide and the lower concentration of Li_2O_2 at the electrode surface in SIS are expected to be beneficial to suppress film growth on the electrode surface and to favor solution formation which, however, also depends on the adsorption strength of Li_2O_2 on the electrode surface. ~~As it concerns reoxidation of ORR products the enhancement of $I_{p,ox}$ at 2m vs 0.5m (Figure 2a) could be attributed to the notable increase of viscosity (31 cP and 7 cP, respectively , see Table 1) that causes an higher confinement of the Li_2O_2 (the oxidation reactant)~~

~~near the electrode surface. At concentrations higher than 2m (Figure 2b), $I_{p,ox}$ does not change because the lower amount of Li_2O_2 at the electrode surface is balanced by the higher solution viscosity. Furthermore, the values of E_{ox} of 2m-5m solutions (3.26, 3.25, 3.27 V vs Li^+/Li) are lower than those of the 0.5m (3.32 V vs Li^+/Li), suggesting that the adsorption of Li_2O_2 on the electrode surface is less efficient at the highest salt concentrations [37].~~

The strength of the interaction of Li_2O_2 with the electrode surface can be evaluated by the analysis of the oxidation peak potentials. A strong adsorption of the oxidation reactant results in a shift towards high potentials of the anodic peak [37]. The values of E_{ox} of 2m-5m solutions (3.26, 3.25, 3.27 V vs Li^+/Li) are lower than those of the 0.5m (3.32 V vs Li^+/Li) and this suggests that the adsorption of Li_2O_2 on the electrode surface is weaker at the highest salt concentrations.

Further insight into the nature of Li_2O_2 formed at the electrode surface can be get by the analysis of the CV peak currents (I_p) with the scan rate (v_{scan}). Indeed, in the case of strongly adsorbed reactants, the peak currents linearly increase with v_{scan} (like for a surface reaction). For processes involving species in solutions and controlled by mass transport, the peak currents linearly increase with the square root of v_{scan} [37].

The CVs at different scan rates and the trends of I_p with v_{scan} in the investigated electrolytes are reported in the SI (Figure 2S and Figure 3S). Table 2 reports the slopes of the Log I_p vs Log v_{scan} plots for the reduction and oxidation peaks ($slope_{red}$ and $slope_{ox}$). The values of $slope_{red}$ are ca. 0.6-0.7 for all the different concentrations of Li^+ salt, confirming that the process is limited by the diffusion of the reactant (e.g. O_2) in solution (Figure 3S a) [37]. Instead, the values of $slope_{ox}$ at the lowest concentrations (0.1m and 0.5m) are ca. 0.9 . This indicates that the anodic process is a surface reaction that can be identified with the oxidation of Li_2O_2 that was

previously formed during the cathodic scan (eq. 6) as a solid product strongly absorbed at the electrode surface [37]. It is worth noting that for the highest concentrations (2, 4 and 5m), the oxidation peak current tends to be proportional to the square root of the scan rate ($slope_{ox}$ decreases to ca 0.7), thus suggesting that in these cases, oxidation is prone to lose the finger print of a surface reaction and be more like a process controlled by mass transport of reactants (Li_2O_2 included) in solution. This is an additional evidence that oxidation reaction in SIS involves particles of Li_2O_2 which are weakly adsorbed on the electrode surface. It supports the idea of a different nature of Li_2O_2 formed at the electrode in the different electrolytes.

All together the above reported observations suggest that Li_2O_2 production process changes from a surface growth to a solution formation mechanism moving from salt-in-solvent to SIS solutions. This conclusion is supported also by the data in Figure 2c that shows the trend of the O_2 reduction charge (Q_{red}) over repeated CV cycles at 20 mV s^{-1} that were performed without cleaning the GCE between subsequent scans: charge retention is higher for 4m and 5m solutions than for 0.5m and 2m. This could be also explained considering that in equimolar solutions no free solvent molecules are present, hence the glyme is less available for degradation side reactions [38]. Therefore, the superconcentrated solutions may improve the Li/O_2 cycling performance.

The high viscosity of 4m and 5m solutions should not be taken as a limit for their use. Indeed, Figure 2 shows that ORR peak currents, hence ORR kinetic rates, are similar to those of the diluted solutions. The peak currents are related to the concentration (C) and diffusion coefficient (D) of O_2, which is the redox active species [39]. It is reasonable to assume that D decreases with electrolyte viscosity and salt concentration increase. Therefore, a corresponding augment of C that balances the mass transport delay is expected. Such increase of C might be explained taking

into account that a higher LiTFSI molality corresponds to a higher fluorine content, which is known to favor O_2 solubility [35, 40, 41].

An accurate voltammetric evaluation of C and D is not possible in the investigated electrolyte set because, as commented above, the mechanism of ORR is prone to change with the lithium salt concentration. Correct C and D values by CV analysis would require specific current functions as proposed by Nicholson and Shain, not available, that take into account the different rate of the irreversible chemical reaction (LiO_2 dismutation, eq. 4) following the electrochemical step (eq. 3) for the various electrolytes [39].

Figure 3 reports the galvanostatic discharge at 0.05 mA cm^{-2} of a Li/O_2 cell with carbon paper cathode, lithium anode and different O_2-saturated LiTFSI-TEGDME electrolytes. The CP was not coated by any porous carbon or catalyst in order to make the system as simple as possible, and to focus the measurement only on any electrolyte effect. The solutions were stirred in order to level and improve the low O_2 mass transport rate which is related to the different viscosity of the media. Note that the use of a flowable O_2 catholyte has been already demonstrated to be a valuable approach to achieve high discharge current in flow Li/O_2 batteries [42, 43]. The CP potentials in Figure 3 increase by 200 mV, i.e. from 2.52 to 2.72 V vs Li^+/Li, moving from 0.5m to 5 m, therefore further supporting a higher solubility of O_2 at the highest salt concentration.

<Figure 3>

The value of C was determined by a non-electrochemical method. Specifically, luminescence studies were performed for the first time to evaluate O_2 solubility in electrolytes for lithium batteries. The luminescent metal complex tris(bipyridine)ruthenium chloride ($Ru(bpy)_3Cl_2$) was

used as a probe since its luminescence intensity and lifetime are largely affected by the presence of O_2 in solution [28, 29].

Figure 4 reports the emission spectra of 10^{-5} M $Ru(bpy)_3Cl_2$ in LiTFSI-TEGDME electrolytes with different LiTFSI concentration and in $PYR_{14}TFSI$ for a comparison. The emission maximum undergoes a blue shift by increasing the lithium salt concentration suggesting a significant interaction among the electrolyte and the ruthenium complex. The increase in the energy of the emission could be reasonably explained by two synergistic effects: i) the electrostatic interaction between the positive ruthenium complex and the negative $TFSI^-$ ions stabilizes the ground state; ii) the excited complex is destabilized by the $TFSI^-$ surrounding anions because in the excited state an electron is transferred to one of the bpy ligands (MLCT).

<Figure 4>

Table 3 reports the photophysical data and the oxygen concentrations calculated by eq. (1) for different LiTFSI-TEGDME solutions and for the $PYR_{14}TFSI$ ionic liquid for comparison.

<Table 3>

Table 3 shows C values of 2.4, 4.1, 4.4, 14, 18 mM for 0, 0.5, 1, 2, 3m LiTFSI, respectively, thus confirming that the increase of fluorinate salt promotes O_2 solubility.

On the basis of the very high viscosity of 5m solution (550 cP), a very slow quenching of the complex should be expected, which is the opposite of what has been observed. Indeed, the lifetime of luminophore in presence of O_2 is almost the same than that measured in the 3m solution with a ten times lower viscosity (47 cP), and in $PYR_{14}TFSI$ IL (60 cP, [35]). This

observation again suggests that kinetics in SIS solutions can be fast. On the other hand, SISs have an IL-like structure and it has been reported that diffusion of gases in ILs, unlike in common dilute solutions, is influenced by free volume and Lewis acid-base interactions rather than by medium fluidity [44]. The weaker are the interactions between the electrolyte cation and the anion, the larger are the interionic voids where the O_2 molecules can slide moving inside the solution [44, 45]. For this reason, the $[Li(glyme)_1]^+TFSI^-$ structure of the 5m solution could promote O_2 diffusion and D could be much higher than what expected by a conventional Stokes-Einstein approach.

4. Conclusions

Salt concentration has an impact on the ORR intermediates and products stability. The voltammetric study suggests that Li_2O_2 formation mechanism is prone to change from a surface to a solution process moving from salt-in-solvent to SIS solutions. Consequently, cycling stability of Li/O_2 batteries might be improved using superconcentrated solutions. O_2 solubility and diffusion in superconcentrated solutions are higher than that expected by a classical approach based on electrolytes polarity and viscosity. They are affected by the fluorine content and IL-like structure of SIS where the free volume is playing a role. High O_2 concentration and diffusion enable high ORR currents and fast kinetics and this is of great importance for future applications of SIS in next generation of lithium and other metal-based air batteries including flow systems. The stability of superconcentrated solutions is high and meets the demand for safe and reliable materials in the energy conversion/storage field.

Acknowledgments

The work was funded by Alma Mater Studiorum ‑Università di Bologna (RFO, Ricerca Fondamentale Orientata). The authors are grateful to Professor Marina Mastragostino for the fruitful discussions and precious suggestions on the analysis of cycling voltammetry results.

Appendix A. Supplementary data

Supplementary data related to this article can be found at http/

References

[1] G. Girishkumar, B. McCloskey, A. C. Luntz, S. Swanson, W. Wilcke, Lithium-Air Battery: Promise and Challenges, J. Phys. Chem. Lett. 1 (2010) 2193.

[2] K. M. Abraham, Electrolyte-Directed Reactions of the Oxygen Electrode in Lithium-Air Batteries, J. Electrochem. Soc. 162 (2015) A3021.

[3] X. Gao, Y. Chen, L. Johnson, P. G. Bruce, Promoting solution phase discharge in Li-O_2 batteries containing weakly solvating electrolyte solutions, Nat. Mater. 15 (2016) 882.

[4] B. D. McCloskey, A. Speidel, R. Scheffler, D. C. Miller, V. Viswanathan, J. S. Hummelshøj, J. K. Nørskov, A. C. Luntz, Twin Problems of Interfacial Carbonate Formation in Nonaqueous Li−O_2 Batteries, J. Phys. Chem. Lett. 3 (2012) 997.

[5] M. M. O. Thotiyl, S. A. Freunberger, Z. Peng, Y. Chen, Z. Liu, P. G. Bruce, A stable cathode for the aprotic Li-O_2 battery, Nat. Mater. 12 (2013) 1050.

[6] D. Aurbach, B. D. McCloskey, L. F. Nazar, P. G. Bruce, Advances in understanding mechanisms underpinning lithium–air batteries, Nat. Mater. 1 (2016) 1.

[7] B. D. McCloskey, D. S. Bethune, R. M. Shelby, G. Girishkumar, A. C. Luntz, Solvents' Critical Role in Nonaqueous Lithium-Oxygen Battery Electrochemistry, J. Phys. Chem. Lett. 2 (2011) 1161.

[8] J. Read, K. Mutolo, M. Ervin, W. Behl, J. Wolfenstine, A. Driedger, D. Foster D. Oxygen Transport Properties of Organic Electrolytes and Performance of Lithium/Oxygen Battery, J. Electrochem. Soc. 150 (2003) A1351.

[9] M. Balaish, A. Kraytsberg, Y. Ein-Eli, A critical review on lithium–air battery electrolytes, Phys. Chem. Chem. Phys. 16 (2014) 2801.

[10] D. Sharon, D. Hirshberg, M. Afri, A. Garsuch, A. A. Frimer, D. Aurbach, Lithium-Oxygen Electrochemistry in Non-Aqueous Solutions, Isr. J. Chem. 55 (2015) 508.

[11] L. Johnson, C. Li, Z. Liu, Y. Chen, S. A. Freunberger, P. C. Ashok, B. B. Praveen, K. Dholakia, J.-M. Tarascon, P. G. Bruce, The role of LiO_2 solubility in O_2 reduction in aprotic solvents and its consequences for Li–O_2 batteries. Nature Chem., 6 (2014) 1091.

[12] B. D. McCloskey, C. M. Burke, J. E: Nichols, S. E. Renfrew, Mechanistic insights for the development of Li–O_2 battery materials: addressing Li_2O_2 conductivity limitations and electrolyte and cathode instabilities, Chem. Commun. 51 (2015) 12701.

[13] V. Gutmann, Solvent Effects on the reactivities of organometallic compounds, Coord. Chem. Rew. (1976) 225.

[14] R. G. Pearson, Hard and Soft Acids and Bases, J. Am. Chem. Soc. 85 (1963) 3533.

[15] K. M. Abraham, Electrolyte-Directed Reactions of the Oxygen Electrode in Lithium-Air Batteries, J. Electrochem. Soc. 162 (2015) A3021.

[16] C. M. Burke, V. Pande, A. Khetand, V. Viswanathan, B. D: McCloskey, Enhancing electrochemical intermediate solvation through electrolyte anion selection to increase nonaqueous Li–O_2 battery capacity, Proc. Natl. Acad. Sci. U S A 112 (2015) 9293.

[17] N. Akhtar, W. Akhtar, Prospects, challenges, and latest developments in lithium–air batteries, Int. J. Energy Res. (2015) 303.

[18] F. Soavi, S. Monaco, M. Mastragostino, Catalyst-free porous carbon cathode and ionic liquid for high efficiency, rechargeable Li/O_2 battery, J. Power Sources 224 (2013) 115.

[19] J. Read, Ether-Based Electrolytes for the Lithium/Oxygen Organic Electrolyte Battery, J. Electrochem. Soc. 153 (2006) A96.

[20] T. Tamura, T. Hachida, K. Yoshida, N. Tachikawa, K. Dokko, M. Watanabe, New glyme–cyclic imide lithium salt complexes as thermally stable electrolytes for lithium batteries, J. Power Sources, 195 (2010) 6095.

[21] S. Tsuzuki, W. Shinoda, M. Matsugami, Y. Umebayashi, K. Ueno, T. Mandai, S. Seki, K. Dokko, M. Watanabe, Structures of [Li(glyme)]+ complexes and their interactions with anions in equimolar mixtures of glymes and Li[TFSA]: analysis by molecular dynamics simulations, Phys. Chem. Chem. Phys.17(2015) 126.

[22] F. Li, T. Zhang, Y. Yamada, A. Yamada, H. Zhou, Enhanced Cycling Performance of Li-O_2 Batteries by the Optimized Electrolyte Concentration of LiTFSA in Glymes, Adv. Energy Mater. 3 (2013) 532.

[23] L. Suo, Y.-S. Hu, H. Li, M. Armand, L. Chen, A new class of Solvent-in-Salt electrolyte for high-energy rechargeable metallic lithium batteries, Nature Comm. (2013) 1.

[24] Y. Yamada, A. Yamada, Review-Superconcentrated Electrolytes for Lithium Batteries. J. Electrochem. Soc. 162 (2015) A2406.

[25] T. Mandai, K. Yoshida, K. Ueno, K. Dokko, M. Watanabe, Criteria for solvate ionic liquids, Phys. Chem. Chem. Phys. 16 (2014) 8761.

[26] S. M. Barrett, C. Wang, W. Lin, Oxygen sensing via phosphorescence quenching of doped metal–organic frameworks, J. Mater. Chem. 22(2012) 10329.

[27] Y. Feng, J. Cheng, L. Zhou, X. Zhou, H. Xiang, Ratiometric optical oxygen sensing: a review in respect of material design, Analyst 137 (2012) 4885.

[28] A. Juris, V. Balzani, F. Barigelletti, S. Campagna, P. Belser, A. Von Zelewsky, Ru(II) polypyridine complexes: photophysics, photochemistry, eletrochemistry, and chemiluminescence, Coord. Chem. Rev. 84 (1988) 85.

[29] C. J. Timpson, C.C. Carter, J. Olmsted, Mechanism of quenching of electronically excited ruthenium complexes by oxygen, J. Phys. Chem. 93 (1989) 4116.

[30] M. Quaranta, S. M. Borisov, I. Klimant, Indicators for optical oxygen sensors, Bioanal Rev. 4 (2012) 115.

[31] J. Jordan, W. Bauer, Correlations between Solvent Structure, Viscosity and Polarographic Diffusion Coefficients of Oxygen, J. Am. Chem. Soc. 81 (1959) 3915.

[32] M. A. Vorotyntsev, V. A. Zinovyeva, M. Picquet, Diffusional transport in ionic liquids: Stokes–Einstein relation or “sliding sphere”model? Ferrocene (Fc) in imidazolium liquids, Electrochim. Acta 55 (2010) 5063.

[33] F. Messaggi, Electrolytes for Li/O_2 batteries: from “salt in solvent” to “solvent in salt”, Master dissertation thesis, 2016.

[34] F. De Giorgio, F. Soavi, M. Mastragostino, Effect of lithium ions on oxygen reduction in ionic liquid-based electrolytes, Electrochem. Comm. 13 (2011) 1090.

[35] S. Monaco, A. M. Arangio, F. Soavi, M. Mastragostino, E. Paillard, S. Passerini, An electrochemical study of oxygen reduction in pyrrolidinium-based ionic liquids for lithium/oxygen batteries, Electrochim. Acta 83 (2012) 94.

[36] C. O. Laoire, S. Mukerjee, K. M. Abraham, E. J. Plichta, M. A. Hendrickson, Influence of Nonaqueous Solvents on the Electrochemistry of Oxygen in the Rechargeable Lithium-Air Battery, J. Phys. Chem. C 114 (2010) 9178.

[37] A. J. Bard, L. R. Faulkner,. Electrochemical Methods: Fundamentals and Applications, John Wiley & Sons, Inc. New York, USA, (2011).

[38] K. Ueno, R. Tatara, S. Tsuzuki, S. Saito, H. Doi, K. Yoshida, T. Mandai, M. Matsugami, Y. Umebayashi, K. Dokko, M. Watanabe, Li^+ solvation in glyme-Li salt solvate ionic liquids, Phys. Chem. Chem. Phys. 17 (2015) 8248.

[39] R. S. Nicholson, R. S.; Shain, I. Theory of Stationary Electrode Polarography Single Scan and Cyclic Methods Applied to Reversible, Irreversible, and Kinetic Systems, Anal. Chem. 36 (1964) 706.

[40] Y. Nishikami, T. Konishi, R. Omoda, Y. Aihara, K. Oyaizu, H. Nishide, Oxygen-enriched electrolytes based on perfluorochemicals for high-capacity lithium–oxygen batteries, J. Mater. Chem. A 3(2015) 10845.

[41] O. Wijaya, P. Hartmann, R. Younesi, I. I. E. Markovits, A. Rinaldi, J. Janek, R. Yazami, A gamma fluorinated ether as an additive for enhanced oxygen activity in Li-O_2 batteries, J. Mater. Chem. A 3(2015) 19061.

[42] S. Monaco, F. Soavi, M. Mastragostino, Role of oxygen mass transport in rechargeable Li/O_2 batteries operating with ionic liquids, J. Phys. Chem. Lett., 4 (2013) 1379.

[43] I: Ruggeri, C. Arbizzani, F. Soavi, A novel concept of semi-solid, Li redox flow air (O_2) battery: a breakthrough towards high energy and power batteries, Electrochim. Acta 206 (2016) 291.

[44] Z. Lei, C. Dai, B. Chen, Gas Solubility in Ionic Liquids, Chem. Rev. 114 (2014) 1289.

[45] J. Jordan, W. Bauer, Correlations between Solvent Structure, Viscosity and Polarographic Diffusion Coefficients of Oxygen, J. Am. Chem. Soc. 81 (1959) 3915.

Figure Captions

Figure 1. Schematic representation of LiTFSI-TEGDME solutions. On the left, a diluted solution; on the right, an equimolar solution with an IL-like structure.

Figure 2. GCE cyclic voltammograms (CVs) at 20 mV s^{-1} in O_2 saturated solutions. (a) 0.1, 0.5 and 2m LiTFSI-TEGDME electrolytes. (b) 2, 4 and 5m LiTFSI-TEGDME electrolytes. (c) O_2 reduction charge (Q_{red}) over repeated CVs at 20 mV s^{-1} between 1.9 V and 4.0 V vs. Li^+/Li for different TEGDME-LiTFSI solutions.

Figure 3. Electrode potential profiles during galvanostatic discharges at -0.05 mA cm^{-2} of CP (0.45 cm^2) and lithium in stirred, O_2-saturated 0.5m, 2m, 4m and 5m electrolytes.

Figure 4. Emission spectra of 10^{-5} M $Ru(bpy)_3Cl_2$ in LiTFSI-TEGDME electrolytes with different LiTFSI concentration and in $PYR_{14}TFSI$.

Figure1

Click here to download high resolution image

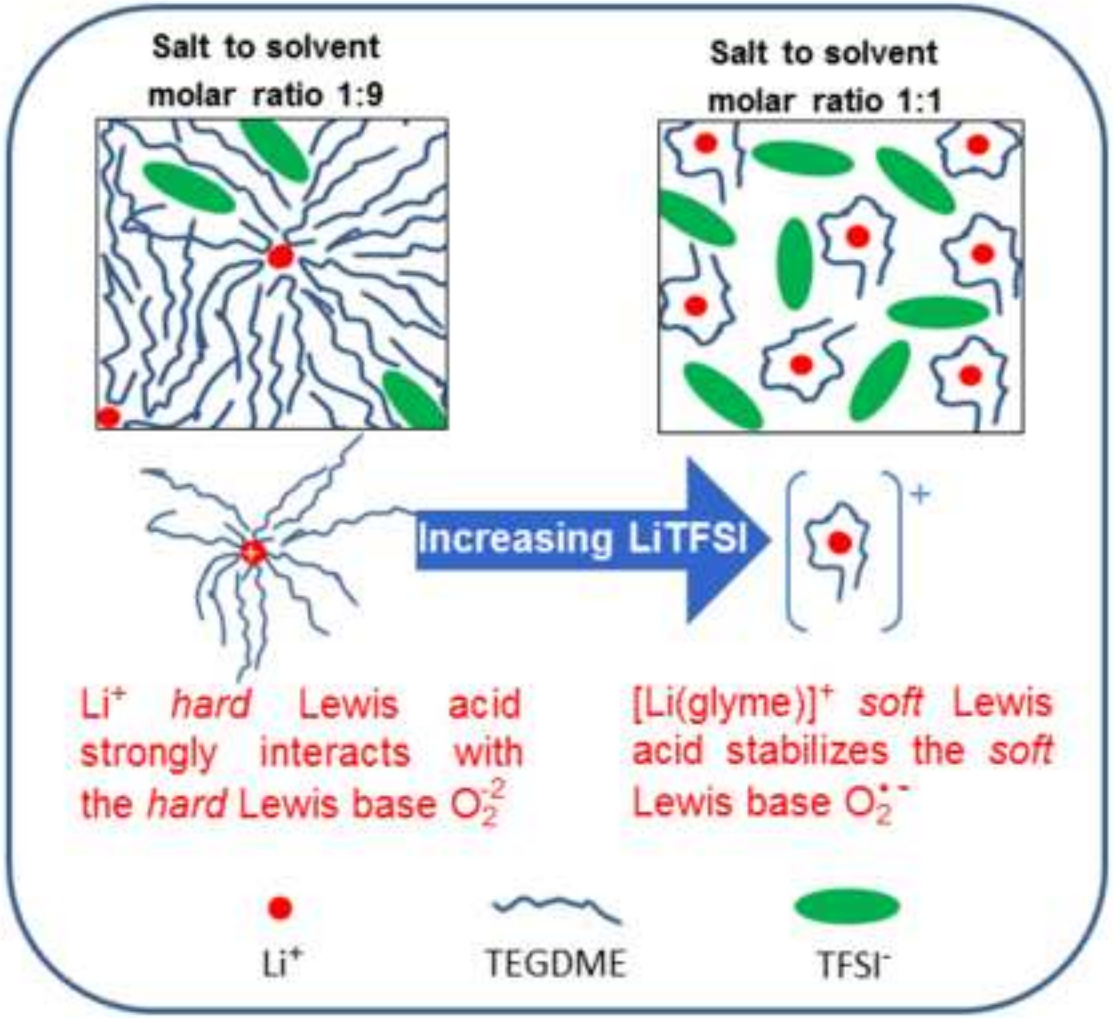

Figure2

Click here to download high resolution image

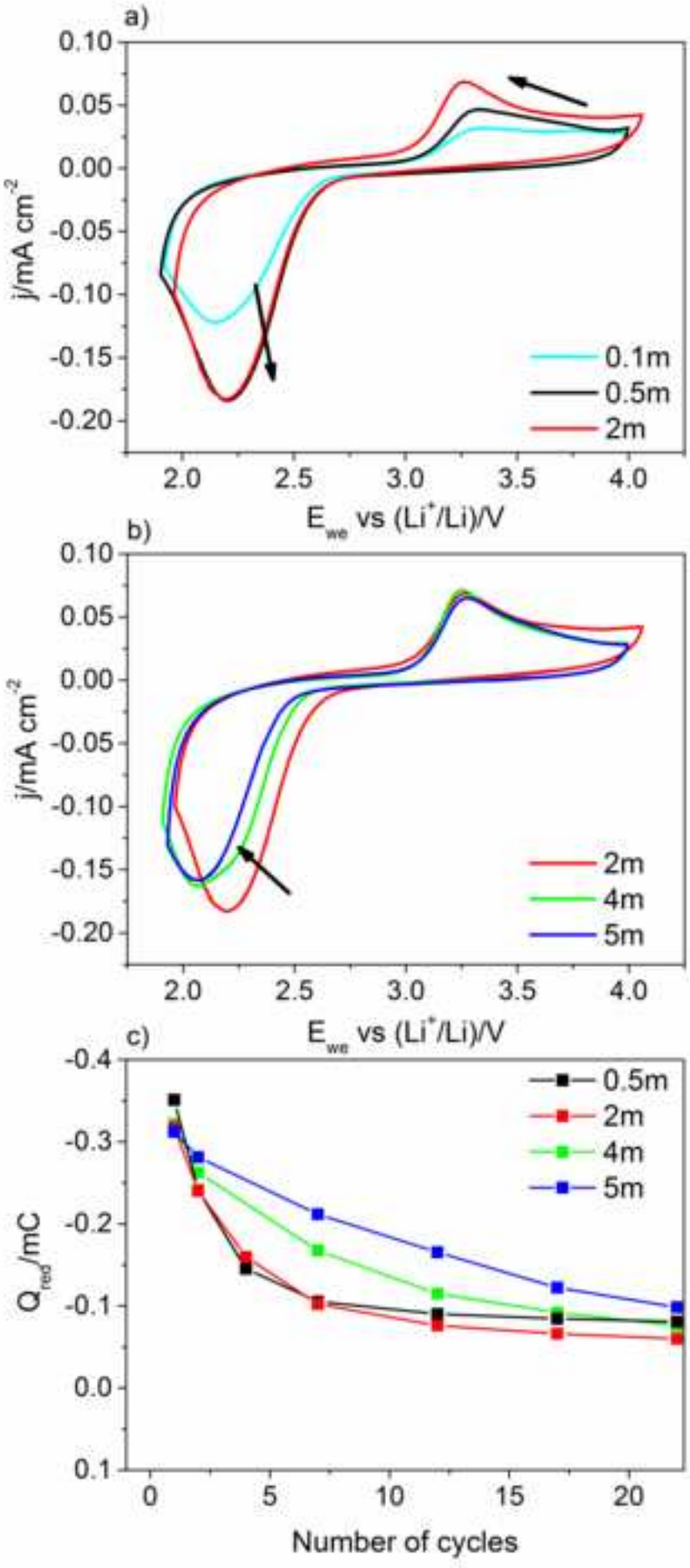

Figure3
Click here to download high resolution image

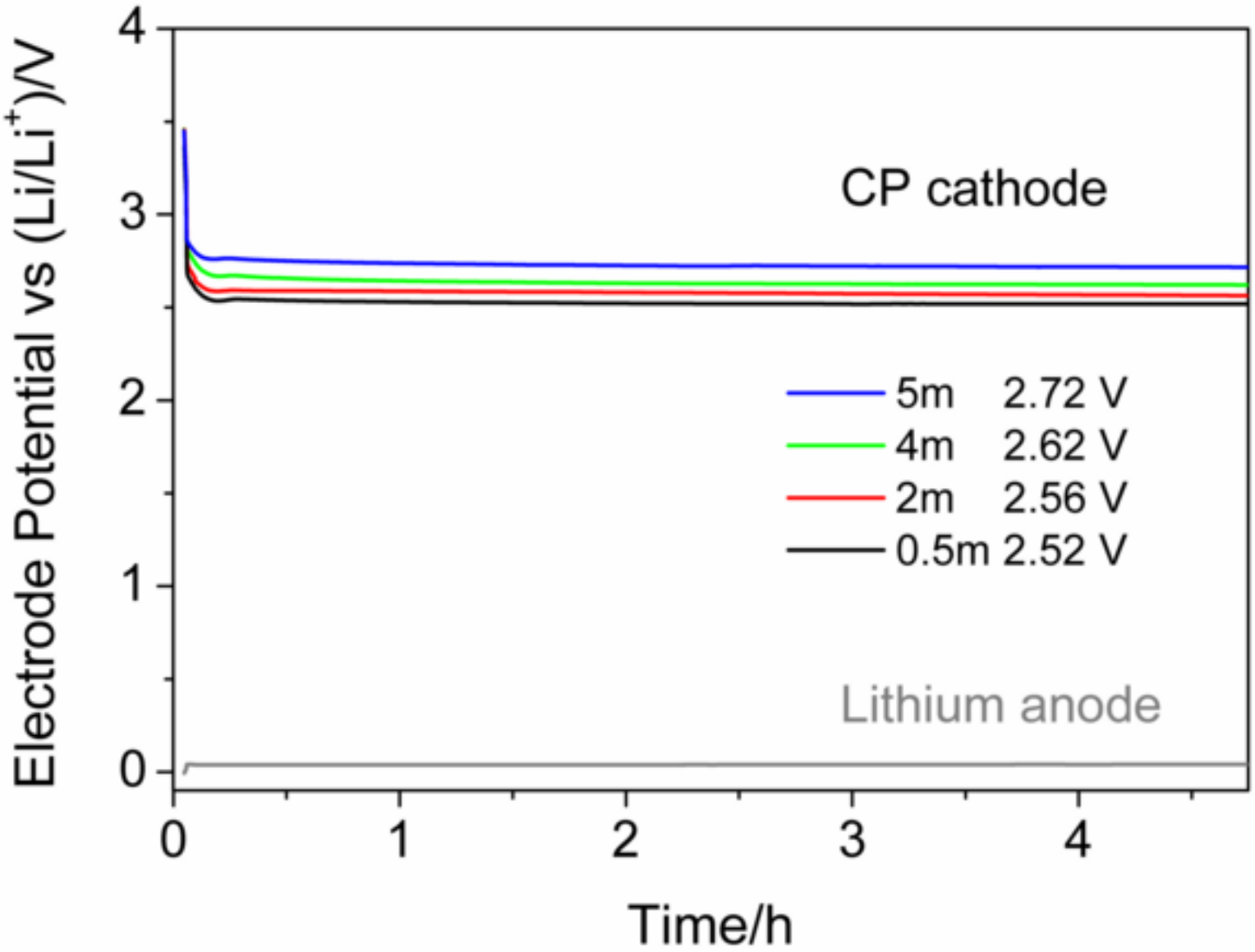

Figure4

Click here to download high resolution image

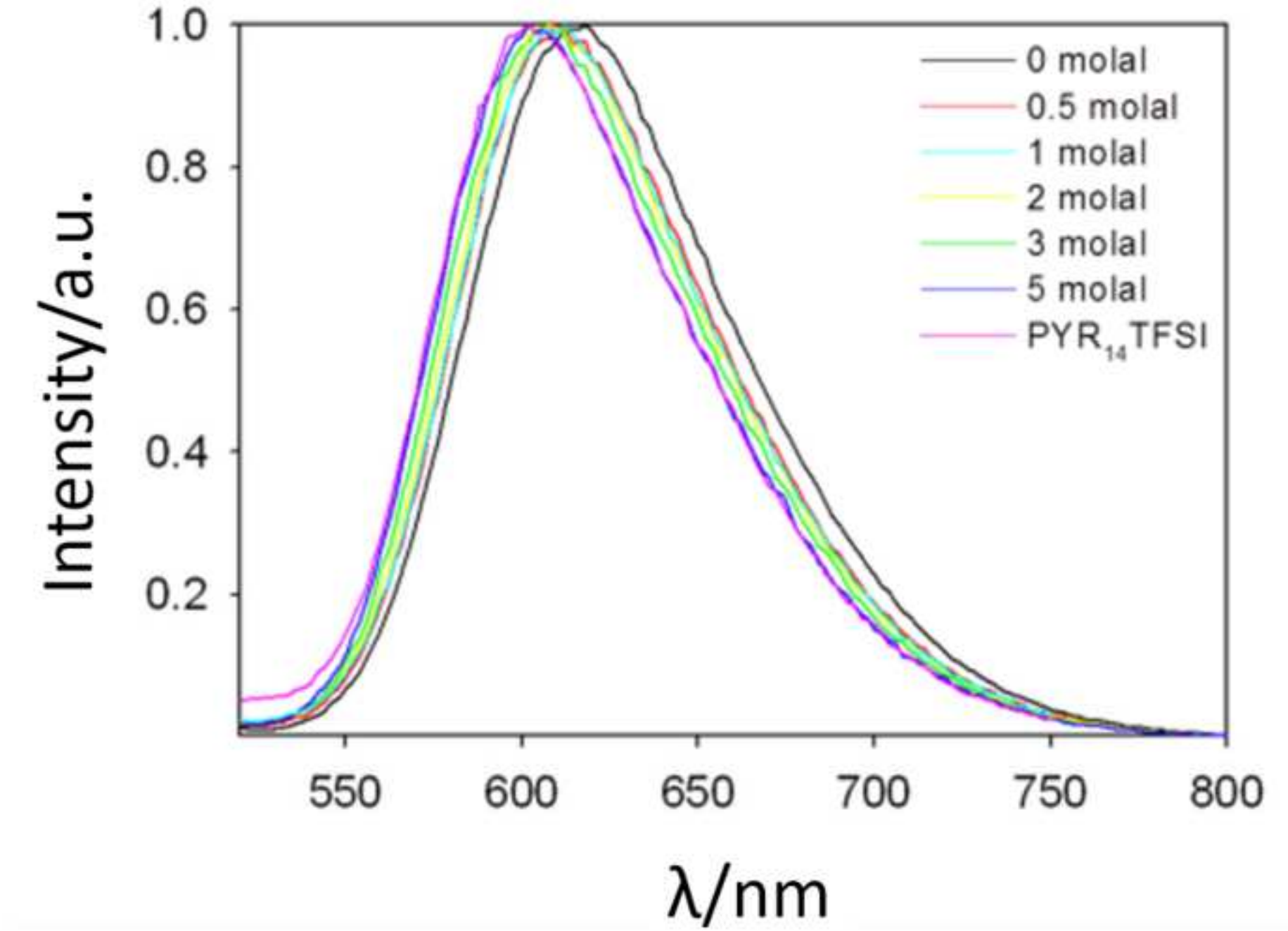

Table1

Table 1. Concentrations, dynamic viscosity, density, conductivity and thermal weight loss temperature (T_d) of the TEGDME-LiTFSI solutions.

	0.5m	**2m**	**4m**	**5m**
Molality *($mol_{salt}/kg_{solvent}$)*	0.5	2.0	4.0	5.0
Molarity *($mol_{salt}/L_{solution}$)*	0.47	1.57	2.56	2.92
Molar ratios (salt to solvent)	1:9.0	1:2.3	1:1.1	1:0.9
Dynamic viscosity (cP)	7.1	31	91	550
Density (g/ml)	1.07	1.24	1.38	1.43
Conductivity (mS/cm)	1.76	1.92	1.43	0.73
T_d (°C)	124	190	243	284

Table2

Table 2. CVs reduction and oxidation peak potentials (E_{red}, E_{ox}), peak currents ($I_{p,red}$, $I_{p,ox}$), reduction charge (Q_{red}), coulombic efficiency (Q_{ox}/Q_{red}) and slopes of Log I_p vs Log v_{scan} plots in reduction ($slope_{red}$) and oxidation ($slope_{ox}$) for the TEGDME-LiTFSI solutions.

	0.1m	**0.5m**	**2m**	**4m**	**5m**
$\mathbf{E_{red}}$ (V vs. Li^+/Li)	2.15	2.2	2.19	2.07	2.07
$\mathbf{E_{ox}}$ (V vs. Li^+/Li)	3.35	3.32	3.26	3.25	3.27
$\mathbf{I_{p\ red}}$ (μA)	2.2	3.3	4.8	5.0	4.6
$\mathbf{I_{p\ ox}}$ (μA)	2.2	3.3	4.8	5.0	4.6
$\mathbf{Q_{red}}$ (mC)	-0.247	-0.349	-0.321	-0.30	-0.276
$\mathbf{Q_{ox}/Q_{red}}$ (%)	43%	38%	65%	53%	57%
$\mathbf{Slope_{red}}$	0.69	0.65	0.67	0.64	0.60
$\mathbf{Slope_{ox}}$	0.88	0.91	0.73	0.74	0.67

Table3

Table 3. Emission wavelength ($\lambda_{emission}$) and lifetimes in absence (τ_0) and presence (τ) of O_2 of 10^{-5} M $Ru(bpy)_3Cl_2$ in different electrolytes: TEGDME-LiTFSI and $PYR_{14}TFSI$. Lifetimes were used to calculate the oxygen concentrations [O_2] by eqs. (1) and (2).

LiTFSI molality	**$\lambda_{emission}$**	**τ_0**	**τ**	**[O_2]**	**Viscosity**
($mol_{salt}/kg_{solvent}$)	(nm)	(ns)	(ns)	(mM)	**η** (cP)
0	618	832	115	2.4	3.6
0.5	610	773	117	4.1	7.1
1	612	735	125	4.4	8.7
2	608	717	144	14	31
3	608	597	156	18	47
5	602	534	172	--	550
$PYR_{14}TFSI$	602	572	156	28	60